Optical and Quantum Electronics (2023) 55:392
https://doi.org/10.1007/s11082-023-04660-9

A novel azo compound derived from ethyl-4-amino benzoate: synthesis, nonlinear optical properties and DFT investigations

Qusay M. A. Hassan[1] · Rafid H. Al-Asadi[2,1] · H. A. Sultan[1] · Hasanain A. Abdullmajed[2] · Asaad A. Ali[2] · C. A. Emshary[1]

Received: 28 August 2022 / Accepted: 6 February 2023

Abstract
A novel azo dye compound, Ethyl (E)-4-((5-hydroxy-3,4-bis(hydroxyl methyl)-6-methyl. pyridin-2-yl)diazenyl)benzoate (EAB), have been synthesized by the coupling reaction and characterized by FT-IR, ^{1}H-and ^{13}C-NMR, Mass, and UV–visible spectroscopies. The nonlinear optical (NLO) properties of the EAB compound via the finding of the nonlinear refractive index (NRI) using continuous wave (cw), low power 473 nm, TEM_{00} mode laser beam have been studied via the diffraction patterns (DPs) and the Z-scan. Effect of power input of the laser beam, types of beam wavefront and temporal variation of the DPs are discussed. The all-optical switching (AOS) using two laser beams is proved to occur in this compound.

Keywords Novel azo dye · DFT · DPs · Z-scan · All-optical switching

1 Introduction

Recently, vast number of researchers are interested in finding and/or preparing systems of high quality that behave nonlinearly towards laser light beams since the index of refraction becomes intensity dependent as it is exposed to electric field of high values. The laser beam interaction with nonlinear materials leads to variety of effects in the transverse dimensions viz., self-focusing (SF) and defocusing (SDF), spatial ring formation, self-phase modulation, etc., (Villafranca and Saravanamuttu 2012; Saeed et al. 2020; Elias et al. 2019, 2018; Emshary et al. 2021a; Ali et al. 2020; Jassem et al. 2021; Shabeeb et al. 2020; Sultan et al. 2021; Mutlaq et al. 2021; Abdullmajed et al. 2022a). Materials having high nonlinear optical (NLO) third-order properties and ultra-fast response time led to considerable scientific activities for their potential applications viz., optical computing, optical phase conjugation,

✉ Qusay M. A. Hassan
qusayali64@yahoo.co.in

[1] Department of Physics, College of Education for Pure Sciences, University of Basrah, Basrah 61001, Iraq

[2] Department of Chemistry, College of Education for Pure Sciences, University of Basrah, Basrah 61001, Iraq

Published online: 07 March 2023

all-optical switching (AOS), holography, spatial dark soliton transmission, optical power limiting, harmonic generation (Al-Hamdani et al. 2021; Khalaf et al. 2022; Emshary et al. 2021b; Qusay et al. 2021; Dhumad et al. 2021a, 2021b; Ruddock 1994; Ambs 2010; Ali and Palanisamy 2007; Manickasundaram et al. 2008a, 2008b, 2011; Ali et al. 2006; Bohac 2010) etc.

Azo compounds are receiving great interests in the scientific research (Kirkan and Gup 2008; Benkhay et al. 2020; Mohammed 2021; Ali et al. 2018), and consumed a great rank in chemical analysis. A powerfully colored azo compound can be red, yellow, orange, blue and sometimes green, based on the molecular structure of the molecules (Otutu 2013). The organic compounds structural features, produces color are, N=O, C=N, N=C, aromatic rings usually, NO_2 and C=O. However, the groups that always grant color are the nitroso (N=O) and azo (–N=N–) (Fayadh et al. 2015). Azo compounds containing one or more azo (–N=N–) groups, are associated with SP^2 hybridized carbon atoms, based on the groups number (Langhals 2004). These azo compounds have the ability to form chelate coordination complexes with more metal ions, characterized by its color and its dissolve ability in different organic and inorganic solvents (Child et al. 1977). Further, the azo compounds are reactive compounds, which were reported for their pharmaceutical importance as antineoplastic, antidiabetic (Tahir et al. 2021), anticancer (Farghaly and Abdallah 2008) and antibacterial (Ali et al. 2018). The theoretical studies on the structure of each synthetic azo compounds were also carried to describe the relation among the molecular structure and the compounds properties (Al-Masoudi et al. 2015; Dhaef et al. 2021).

The purpose of the present work was to synthesize a new azo dye (EAB) compound through the coupling reaction between ethyl-4-amino benzoate and (5-hydroxy-6-methylpyridine-3,4-diyl)dimethanol and study some electronic characteristics using of computational chemistry calculations. Also EAB compound NLO properties were investigated using a continuous wave (cw) low power, TEM_{00} mode, laser beam of 473 nm wavelength where the azo dye (EAB) nonlinear refractive index (NRI) was calculated based on diffraction patterns (DPs) and the Z-scan. AOS was studied in the azo dye (EAB) compound via two beams controlling, 473 nm, and controlled, 532 nm laser.

2 Experimental

2.1 Instrumentation and methods

Reagents and solvents were obtained from Merck and Aldrich, used without purification. Infrared spectrum was recorded as KBr discs, and using a SHIMADZU FT-IR-8400S. The compound melting points were measured using a thermo Scientific (9100). The compound, ^{1}H-and ^{13}C-NMR, spectra were obtained using a Bruker 500 MHZ at 25 °C in solvent DMSO. UV–visible spectrum was measured by JENWAY 6305 spectrophotometer in ethanol solvent of 1×10^{-3} molar concentration. Mass spectrum was measured by E1 Technique, using Agilent Technologies spectrometers and using 70 eV.

2.2 Preparation of ethyl (E)-4-((5-hydroxy-3,4-bis(hydroxyl methyl)-6-methylpyridin-2-yl) diazenyl)benzoate (EAB).

(0.006 mol., 0.9911 g) of Ethyl-4-amino benzoate was dissolved in solution of 2 mL of conc. HCl and 8 mL of deionized distilled water. An $NaNO_2$ solution prepared as the first

solution by dissolving 0.456 g in 5 mL of distilled water, solution of $NaNO_2$ as the second solution was added gradually to the first solution keeping the mixture temperature in the range 0–5 °C. The resulting diazonium salt was gradually added to a solution (0.006 mol., 1.009 g) of 5-hydroxy-6-methylpyridine-3,4-diyldimethanol dissolved in 10 mL of sodium hydroxide solution 25%. The final mixture was stirred for one hour in an ice bath at a temperature not more than 5 °C. The resulting red crudes were recrystallized in hexane and ethanol to yield (86%), m.p: 162–164 °C. FT-IR (KBr, ν, cm^{-1}): 2500 and 3286 (O–H), 2989 (C–H aliph.), 1707(C=O), 1602(N=N), 1560(C=C), 1282(C–N), 1234(C-O). ^{1}H-NMR (DMSO, 500 MHz, δ ppm): 11.01(s, 1H, OH), 7.68(d, 2H, $H_{a,a'}$), 6.58(d, 2H, $H_{b,b'}$), 6.10(s, 2H, $H_{c,c'}$), 4.53(q, 2H, O-CH_2), 3.18(s, 4H, Ar-CH_2). 1.25(t, 6H, Ar. and aliph-CH_3). ^{13}C-NMR (DMSO, 500 MHz, δ ppm): 171.8(C_{16}, C=O), 165.13(C_5, C=N), 160.13(C_2, C–O), 154.74(C_1, C–N), 150.05–122.01($C_{3,10,13,12,14,4,11,15}$, C=C), 60.97($C_{18}$, O-$CH_2$), 55.66($C_{22}$+$C_{24}$, C–OH), 18.60,14.20 ($C_{7,19}$, CH_3). MS (EI, m/z%): 344 (M^+, 90). UV–vis. in Ethanol, λ_{mas} (nm): 360, 470.

2.3 Computational Study

The EAB compound structure geometry full optimization and the calculation of the energies of the prepared EAB compound using the DFT approach at the BLYP-level (Abdel-Kader et al. 2021) and DNP was used as a basis set. The UV–visible theoretical spectrum was calculated using TD-DFT method at same level and basis set. All calculations were performed using ver. 5.5 software of Material Studio DMol3-program (Dhaef et al. 2021).

2.4 Diffraction patterns

The DPs were obtained using a usual set-up (Al-Timimy et al. 2020), a solid state laser device emitting a cw 1.5 mm (at e^{-2}) spot size and 473 nm wavelength beam. For the sake of focus the beam on the glass sample cell of 0.1 cm thickness, a positive glass lens of 50 mm focal length, was used, a power meter. A 30×30 cm semitransparent screen 90 cm away from the sample cell was used to cast the resulted DPs and registered by a digital camera was used.

2.5 Z-scan

Z-scans were obtained using the 473 nm beam. The sample was translated a distance (-z)-(+z) where the lens focus situated at z=0. The closed (C) and open (O) aperture (A) Z-scans were conducted by measuring the transmitted beam power through a 2 mm diameter iris and when the iris replaced by another positive lens respectively.

2.6 All-optical switching

The AOS usually conducted with two laser beams, either by collinear, passing one through compound technique (Shen et al. 2019) or by cross passing (Jia et al. 2018, 2019; Shan et al. 2014). The setup consists of two cw laser beams of wavelength 473 nm which initiate ring patterns and 532 nm. Sample glass cell, two power meters, a 50×50 cm semitransparent screen and a digital camera were used.

3 Results

3.1 Synthesis

The current work defines the synthesis of novel azo dye (EAB) compound by coupling reaction between ethyl-4-amino benzoate and 5-hydroxy-6-methylpyridine-3,4-diyldimethanol, represented in Fig. 1. The synthesized compound chemical structure was confirmed by data of FT-Infrared, ^{13}C-NMR, ^{1}H-NMR, and mass spectra where the spectral information agree with expected structure.

The FT-IR spectrum of azo compound exhibited two bands at 3500 and 3286 cm^{-1}, due to O–H groups stretching vibration. A strong band appears at 1707 cm^{-1} assigned to v(C=O) group. The formation of azo group was indicated through the appearing of (N=N) stretching vibration at 1602 cm^{-1}, while the stretching vibration of the C=C group appeared in the form of a medium-strength at 1560 cm^{-1}. In addition, the other bands mentioned in the experimental section, as presented in Fig. 2.

The spectrum of ^{1}H-NMR of EAB compound, Fig. 3, demonstrated a singlet signal at 11.01 ppm attributed to proton of aromatic hydroxyl group. The aromatic protons (H_a, $H_{a'}$) and (H_b, $H_{b'}$) were shown as two doublet signals at 7.68 and 6.58 ppm, respectively. While the protons of aliphatic hydroxyl group (H_c and $H_{c'}$) appeared as a singlet signal at 6.10 ppm. The aliphatic protons of the methylene groups appeared as a quartet signal at 4.53 ppm in position d and as a singlet signal at 3.18 ppm in positions e+e'. Also the spectrum showed triplet and singlet signals at 1.25 ppm assigned to aromatic and aliphatic methyl groups. The ^{13}C-NMR spectrum, Fig. 4, supported the skeletal structure of the azo compound, see the preparation section of the compound.

The molecular ion peak of the EAB compound was seen in the mass spectrum at m/z=344 with 18% abundance, which correspond to $[C_{17}H_{19}N_3O_5]^+$ species, see Fig. 5.

The EAB compound UV–visible spectrum prevailed two peaks (Fig. 6), the first peak appeared at 360 nm belongs to phenyl rings π-π* electronic transition. The second peak appeared at 470 nm is belong to conjugated azo group π-π* electronic transition with phenyl

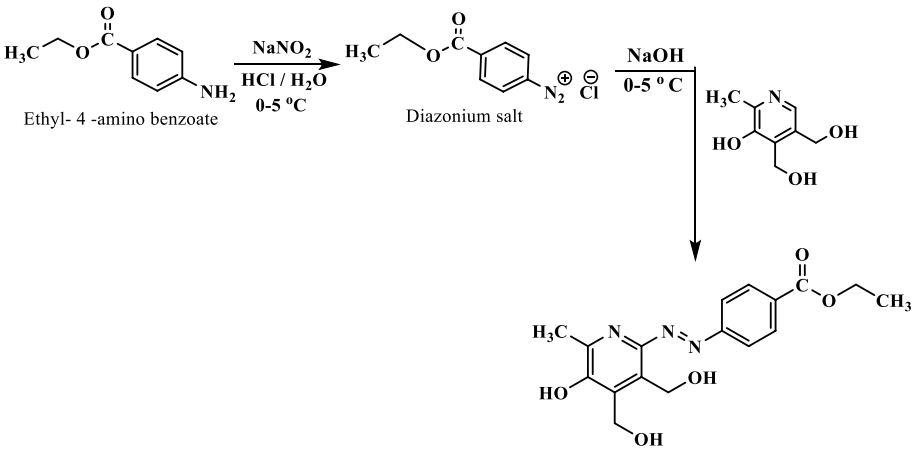

Fig. 1 Synthesis route of the EAB compound

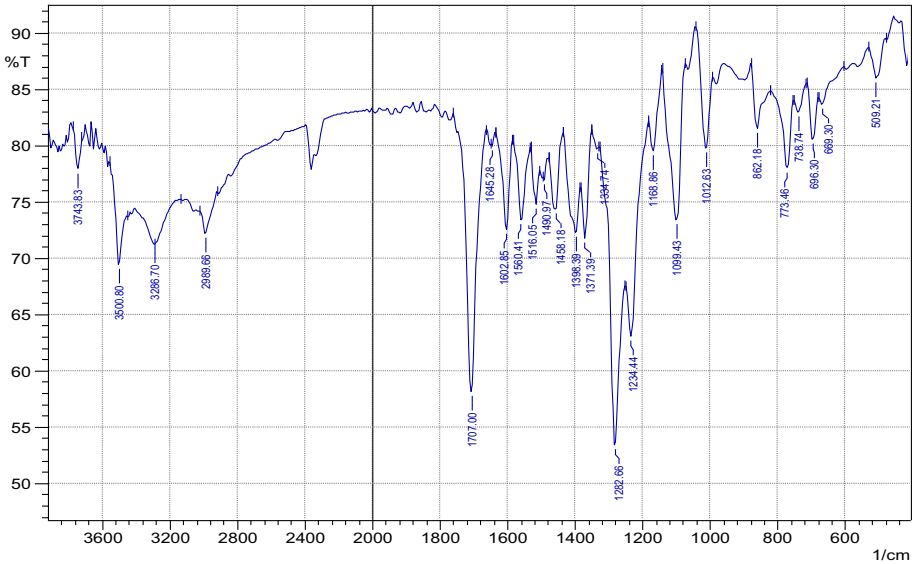

Fig. 2 The EAB compound FTIR spectrum

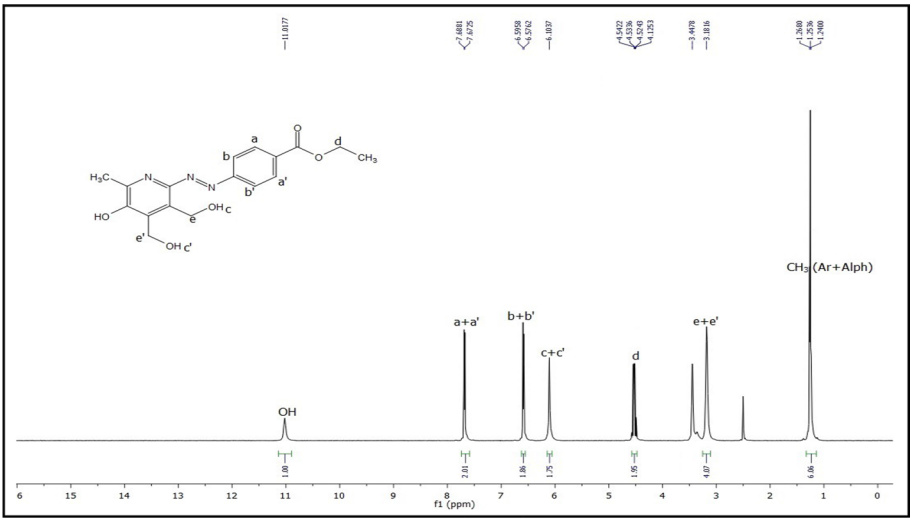

Fig. 3 The EAB compound ^{1}H-NMR spectrum

rings (Sidir et al. 2011). Due to the absorbance (A_i) spectrum at wavelength, λ, the linear absorption coefficients, α_i, can be determined via the equation (Abu El-Fadl et al. 2005):

$$\alpha_i = 2.303\frac{A_i}{d} \quad (1)$$

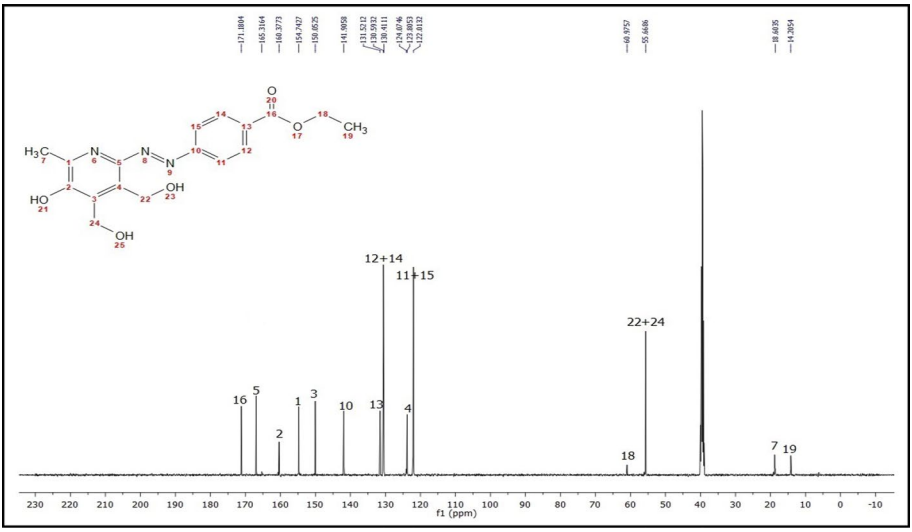

Fig. 4 The EAB compound ^{13}C-NMR spectrum

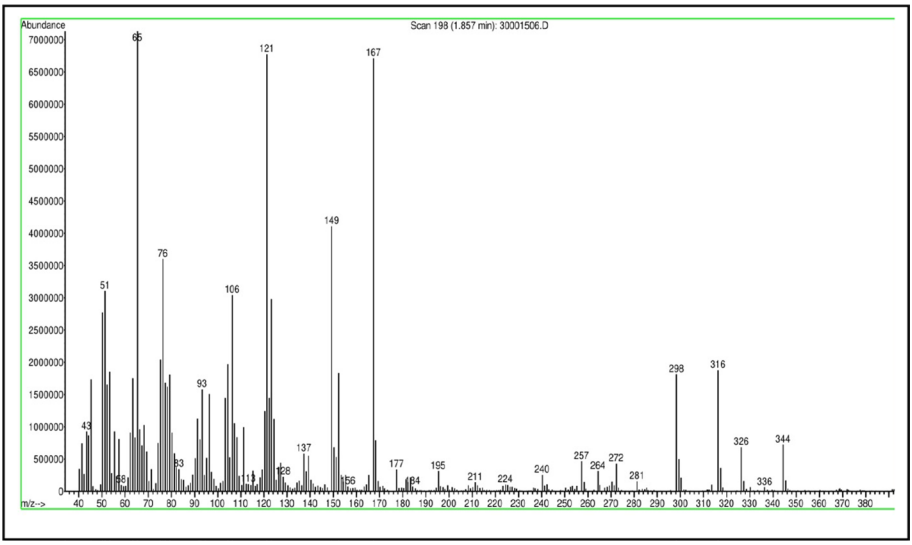

Fig. 5 The EAB compound Mass spectrum

d is the EAB compound thickness so that for $A_{473}=0.68$, $A_{532}=0.233$ and $d=0.1$ cm, $\alpha_{473}=15.66\ \text{cm}^{-1}$ and $\alpha_{532}=5.36\ \text{cm}^{-1}$.

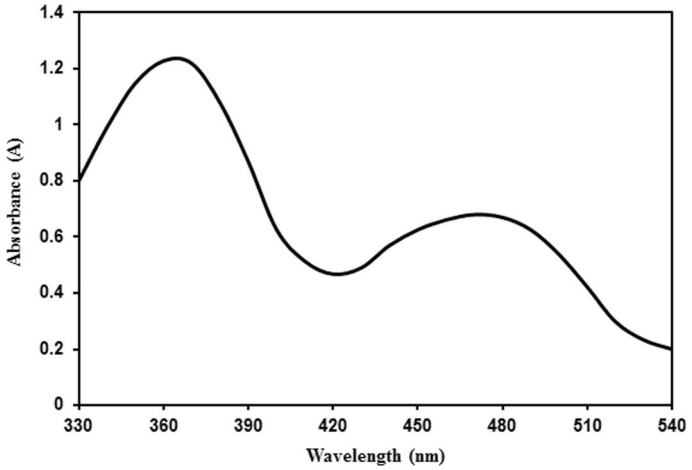

Fig. 6 The EAB compound UV–visible spectrum

3.2 Theoretical studies

3.2.1 Optimization and energies calculations

The optimization of geometry of EAB compound structure was implemented using the DFT method, BLYP level of method and DNP as a basis set. Figure 7 represents the full optimized geometry of the studied EAB compound structure. Total energy, binding energy, HOMO and LUMO energies, ΔE (LUMO–HOMO) and dipole moment value of azo compound were extracted and data are collected in Table1.

The high total energy values and binding energy indicate a better stability of compounds (Al-Asadi 2020). LUMO and HOMO energy and gap energy give expression of the chemical action of molecules, and the molecule which has a small gap energy (LUMO–HOMO) can be linked to high chemical reactivity (Mishra and Tewari 2019). The dipole moment

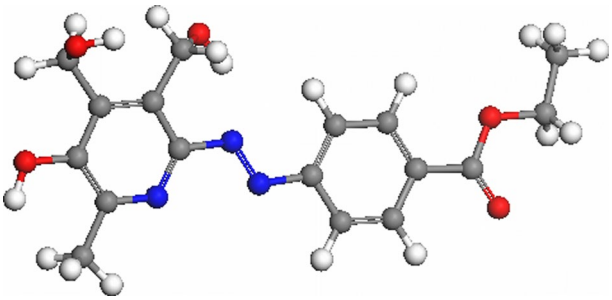

Fig. 7 Optimized structure of the EAB compound

Table 1 Energies and dipole moment values of EAB compound calculated by DFT/BLYP/DNP

Egap (eV)	ELUMO (eV)	EHOMO (eV)	μ (Debye)	Binding energy (eV)	Total energy (eV)
1.847	− 3.301	− 5.148	4.076	− 176.757	− 27,232.378

(μ) is used to find out the molecules polarity, when the electronegativity of atoms increases, the value of dipole moment increases too (Dadrass and Rahchamani 2016). Due to the data in Table 1, we found that the EAB compound has a high stability and chemical activity capability.

3.2.2 Calculated UV–visible spectrum

The EAB compound theoretical electronic transitions spectrum was computed by TD-DFT, BLYP level and DNP basis set using solvent ethanol. In Fig. 8 the UV–vis. spectrum two peaks appeared in accord with the experimental spectrum of the EAB compound, Fig. 6. The EAB computed electronic transitions of excited states are given in Table 2. First peak appeared at 442 nm belong to the electronic transition level between HOMO, 89, and LUMO, 92, with oscillator strength (*f*) value equal 0.713743, this peak belongs to electronic $\pi \rightarrow \pi^*$ transition of conjugated N=N group with phenyl rings. Second peak lies at 348 nm belongs to electronic transition level between HOMO, 83, and LUMO, 92, with oscillator strength (*f*) value equal 0.117524 is assigned phenyl rings $\pi \rightarrow \pi^*$ electronic transitions.

3.2.3 Theoretical calculations of nonlinear optical properties of the EAB compound.

NLO properties of EAB compound have been studied by calculating some chemical global reactivity descriptors (CGRDs) and using urea compound as a reference (Abdullmajed et al. 2022b). The CGRDs calculations are an important way to examine the NLO properties for molecules, such as HOMO energy, electron affinity (EA), global softness (S), and absolute softness (σ). Increasing these parameters can increase the ONL properties of the EAB compound. On the contrary, the chemical hardness (η), energy gap (ΔE), the increase of LUMO energy, and ionization potential (IE) lead to decreasing of NLO properties (Ghanavatkar et al. 2020).

The GCRDs used in the study were calculated according to the following equations (Alharis et al. 2021):

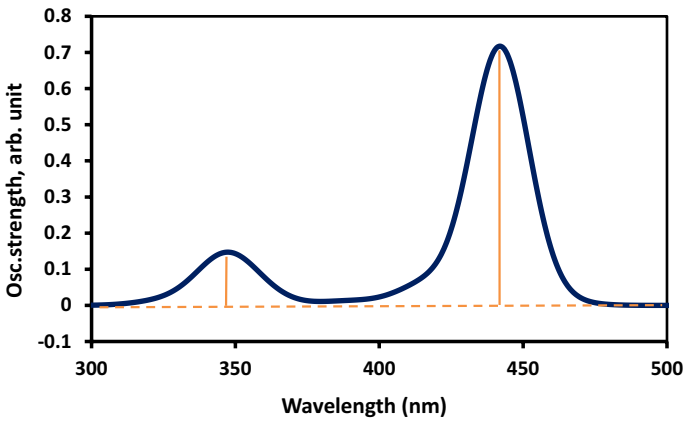

Fig. 8 Calculated UV–visible absorbance spectrum of the EAB compound

Table 2 The excited states of EAB compound using TD-DFT / BLYP / DNP

HOMO → LUMO		State	TD-ex Energy [eV]	TD-ex[nm]	f	Exp. [nm]
From	To			λ_{max}		λ_{max}
91 → 92		1	2.15	576	0.002296	470
90 → 92			2.68	463	0.009036	
89 → 92			2.80	442	0.713743	
88 → 92			2.97	417	0.057823	
87 → 92			3.06	405	0.001936	
86 → 92		2	3.10	401	0.002720	360
85 → 92			3.19	388	0.010635	
84 → 92			3.46	358	0.024595	
83 → 92			3.56	348	0.117524	
91 → 93			3.61	344	0.055589	
90 → 93			3.80	326	0.002508	
82 → 92			3.82	325	0.009699	

$$\begin{aligned}
\text{Energy gap } \Delta E &= (E_{\text{LUMO}} - E_{\text{HOMO}}) \\
\text{Ionization potential IP} &= -E_{\text{HOMO}} \\
\text{Electrone affinity } EA &= -E_{\text{LUMO}} \\
\text{Electonegativity } \chi &= -1/2(E_{\text{HOMO}} + E_{\text{LUMO}}) \\
\text{Chemical hardness } \eta &= -1/2(E_{\text{HOMO}} - E_{\text{LUMO}}) \\
\text{Absolute softness } \sigma &= 1/\eta \\
\text{Global softness } S &= -1/2\eta
\end{aligned}$$

When examining the NLO properties data of the azo compound in Table 3, we note that the values of E_{HOMO}, σ and S for EAB compound are high compared with its values for urea compound. On the other hand, the E_{LUMO}, ΔE and η values of the EAB compound are lower than the urea compound. The obtained results indicate that the EAB compound has high NLO properties compared with the reference urea, see the results in Table 3.

3.3 Diffraction patterns

Figure 9 shows resulted DPs in the far-field with increasing the power input in the range 0–66 mW. These patterns were obtained when sample cell to the screen distance was 85 cm. When the input power was low, a solid bright disc appeared which increase in

Table 3 The GCRD values of EAB and urea compounds, computed at DFT/BLYP/DNP

Compound	E_{HOMO} (eV)	E_{LOMO} (eV)	ΔE (eV)	EA (eV)	IP (eV)	χ (eV^{-1})	η (eV^{-1})	σ (eV)	S (eV)
EAB	−5.148	−3.301	1.847	3.301	5.148	4.224	0.923	1.082	−0.461
Urea	−5.609	0.266	5.875	−0.266	5.609	2.672	2.938	0.340	−1.469

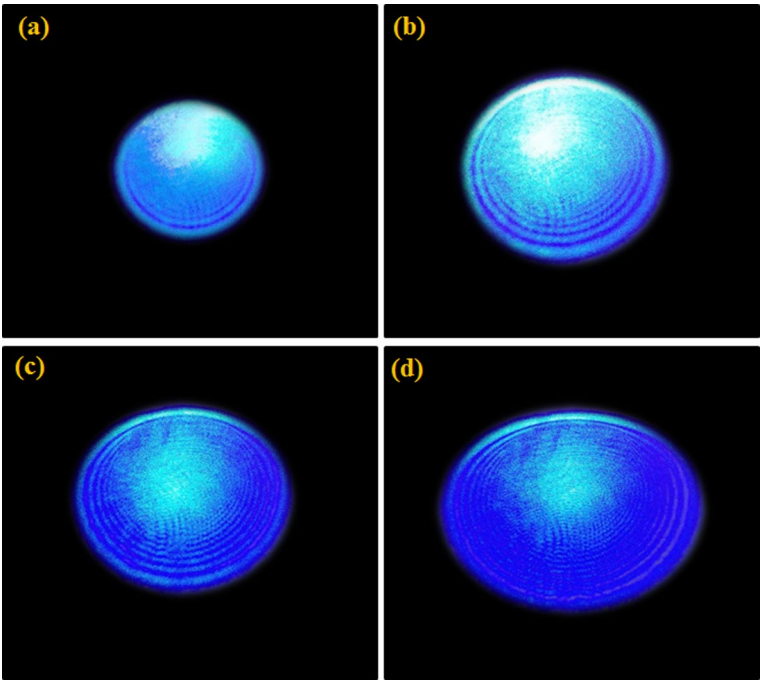

Fig. 9 Images of the DPs evolution in the far field at beam power input (mW): **a** 12, **b** 34, **c** 50, **d** 66, in the EAB compound

area as the power input increased due to self-defocusing (SDF), then breaks into rings. The rings number increased, and the diffraction ring area increases monotonically as power input increased. Up to a certain input power the ring patterns shows symmetry in the (x,y) plane. The pattern top half started to lose symmetry i.e. rings diameters grew less than the lower one i.e., vertically with respect to the horizontal direction. When the ring patterns continues to increase horizontally with increase of input power slowly while vertically it increase first slowly with input power then decreases, i.e., the patterns upper half appear compressed. Figure 10 shows the laser beam curvature type effect i.e. convex and concave on the ring patterns i.e. the beam interaction with the EAB compound is a function of the beam wave front. The temporal evolution of a chosen pattern is shown in Fig. 11; it can be seen that the rings patterns evolve from solid, circular disc to full symmetric patterns up to a certain time, the patterns started to loses symmetry in the upper half depending on the level of input power.

When the phase change in the beam, $\Delta\varphi$, due to the propagation in a nonlinear medium, equals 2π radians, a single ring appear. When rings number, N, at the maximum beam power input, p, the cell thickness of medium was d the beam radius, ω, at the ample cell entrance the NRI, n_2, is given by Ogusu et al. (1996):

$$n_2 = \left(\frac{\pi}{2}\right)\frac{N\lambda\omega^2}{pd} \tag{2}$$

For N = 12, d = 1 mm, $\lambda = 473$ nm, $\omega = 19.235$ µm, p = 66 mW, so that $n_2 = 4.9955 \times 10^{-7}$ cm^2/W.

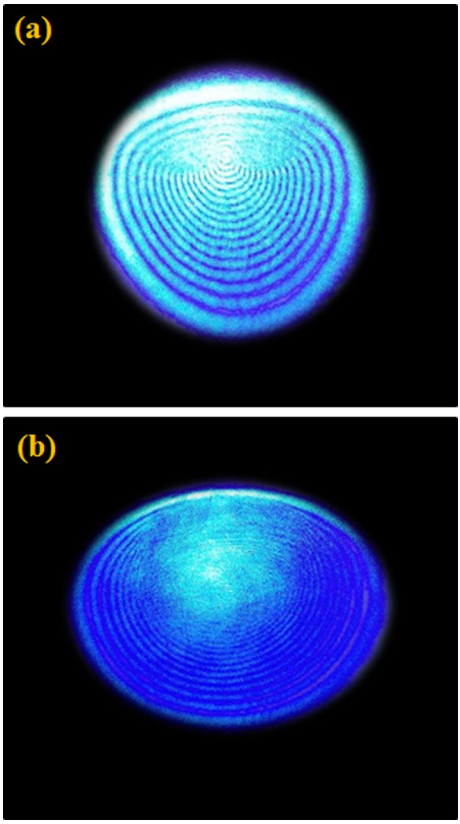

Fig. 10 Images of far field dependence of a chosen DR on the laser beam wavefront **a** convex and **b** concave in the EAB compound at input power 66 mW

3.4 Z-scan

The results of CA Z-scan are shown in Fig. 12a, where a peak succeeded with a valley, resulted an indication that NRI sign is negative, i.e. the beam has SDF. The OA results of Z-scan are shown in Fig. 12b, where a peak value appeared at z = 0, reveal that the sample nonlinear absorption coefficient sign is negative, i.e. the occurrence of saturation absorption. For the sake of obtaining the pure NRI,

data of Fig. 12a must be divided by data of Fig. 12b. The result of the division process is shown in Fig. 12c. The nonlinearity of the EAB compound is thermal since the beam was continuous.

Based on the previous discussion, the Sheik-Bahae model can be used to determine the NRI, n_2, using the following formula (Sheik-Bahae et al. 1989, 1990):

$$n_2 = \frac{\Delta\varphi\lambda}{2\pi L_{eff} I} \tag{3}$$

$\Delta\varphi$ is the laser beam total change of phase, L_{eff} is the sample effective thickness. For beam intensity I = 860 W/cm^2, λ = 473 nm so that $n_2 = 2.55 \times 10^{-7}$ cm^2/W.

The NAC, β, can be determined using the following formula (Matsuoka et al. 1997; X.–j. Zhang et al. 2019)

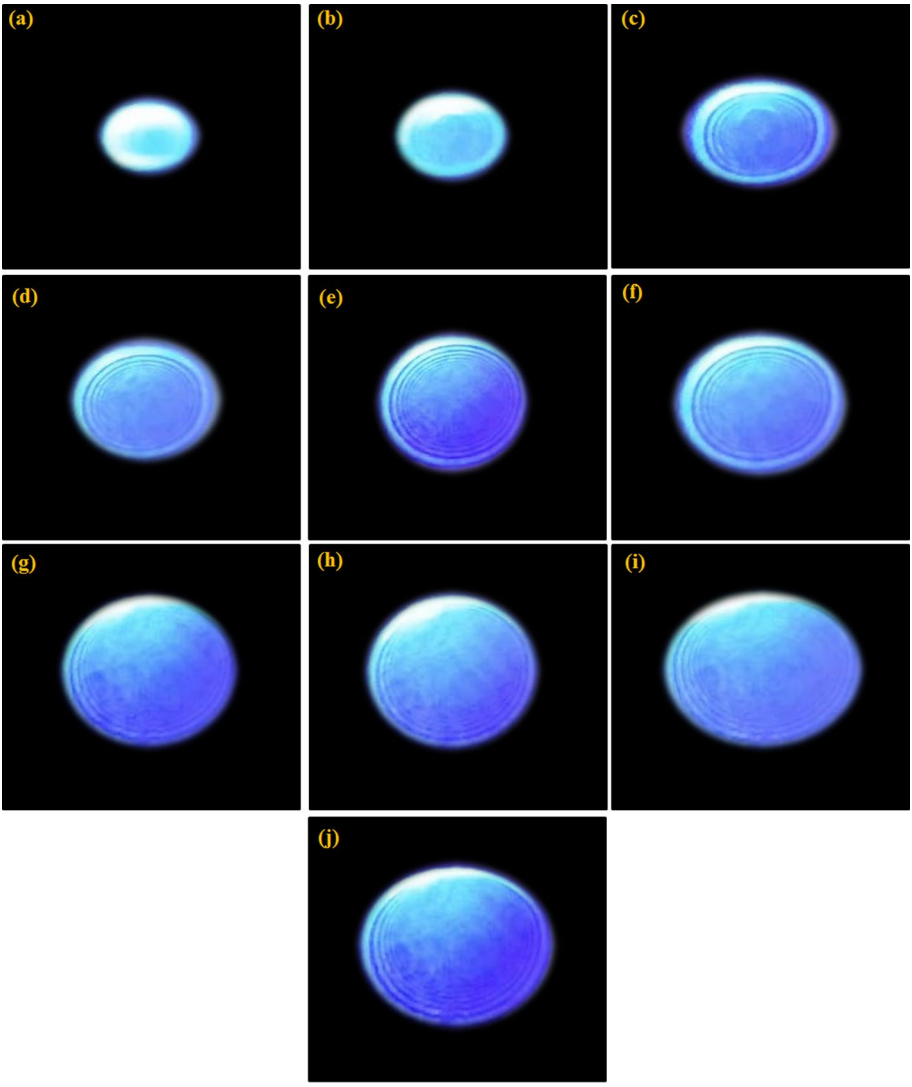

Fig. 11 Images of temporal evolution in the far field of a chosen DP in the EAB compound for power input 66 mW, (msec) **a** 0, **b** 100, **c** 250, **d** 350, **e** 550, **f** 700, **h** 850, **i** 900, **j** 1000

$$\beta = \frac{2\sqrt{2}\Delta T}{L_{eff} I} \tag{4}$$

$\Delta T = 1 - T_p$, where T_p is transmittance peak in the OA Z-scan curve; by using Eq. 4 and Fig. 12b we found the value of $\beta = 3.15 \times 10^{-3}$ cm/W.

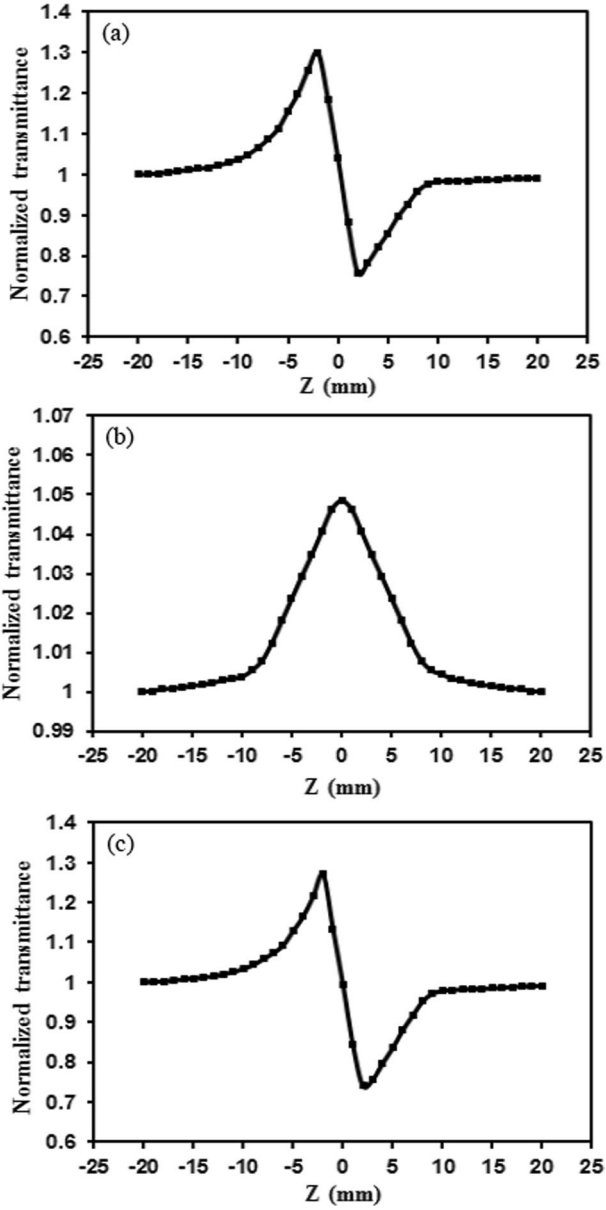

Fig. 12 The laser beam normalized transmittance through the EAB compound versus the sample position (z) with respect to the lens focus (z = 0), **a** CA and, **b** OA, Z-scan, and **c a / b** ratio

3.5 All-optical switching

In this part of experiment, a technique is demonstrated using light beam to control another beam based on the self-cross phase modulation (SXPM) (Agrawal 1987; Matsuoka et al. 1997; Jones et al. 2000; X.–j. Zhang et al. 2019). It is well known that a nonlinear medium of high nonlinear refractive index enhance diffraction patterns when the input intensity exceeds a threshold value when the absorption coefficient is high enough. When using another laser beam of different wavelength where the absorption coefficient of the same medium is low, no

ring patterns appeared. The first controlling strong laser beam of wavelength laser 473 nm where ring patterns appeared when it traverses the EAB compound where the absorption coefficient is high as we saw in the subsection (3.3). Using another laser beam of wavelength 532 nm, controlled one, where the medium has low absorption coefficient, no ring patterns appeared. The results are shown in Fig. 13a. It was noted that the beam controlling affect the area of its DPs patterns, their number of rings, asymmetry and their intensity, while increasing the intensity of the controlling beam does not affect the intensity of controlled beam DPs only. Increasing the intensity of the controlled beam affect the intensity of its DPs alone.

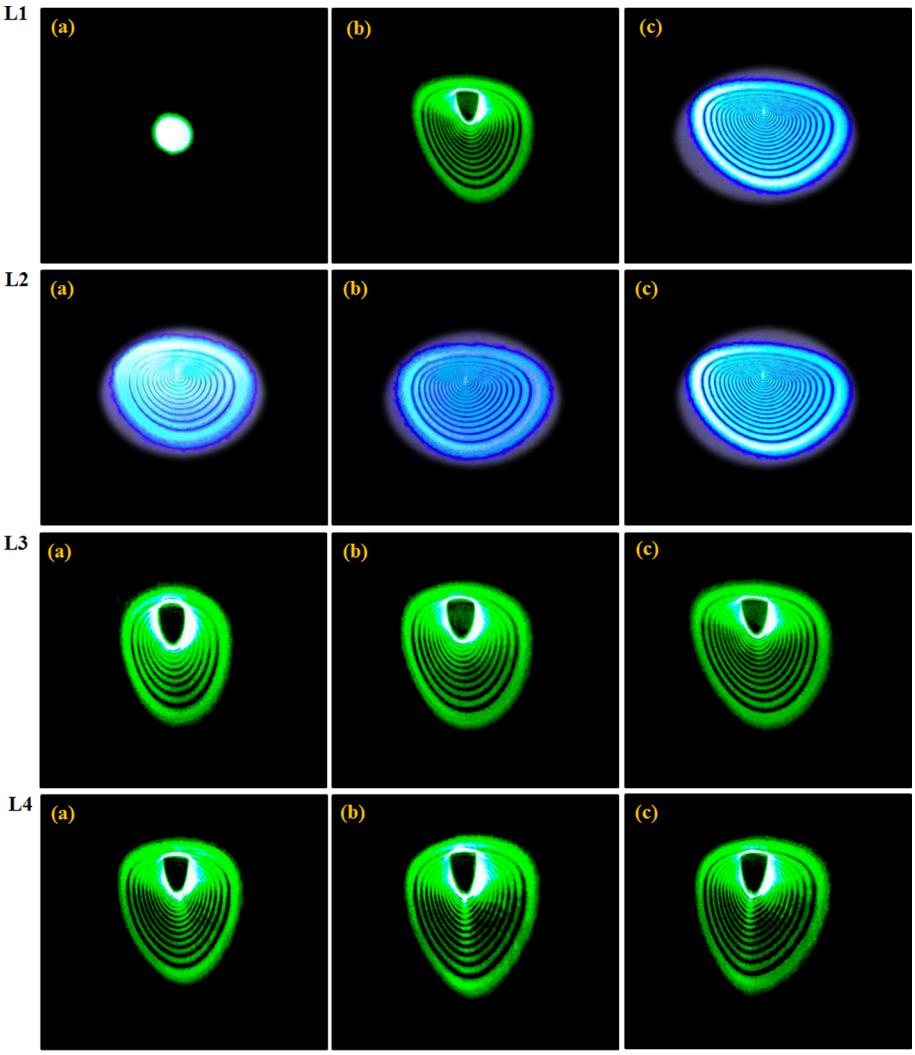

Fig.13 L1 **a** when the controlled 532 nm beam traverses the EAB compound, alone, no rings appeared but a solid spot only. L1 (b+c) when the controlling and the controlled beams traverses the EAB compound two types of DPs appear one for each laser beam. The controlling beam effect on its diffraction ring patterns (L2) while (L3) shows the effects of the controlling beam on the controlled beam DPs and (L4) shows the controlled laser beam effect on its DPs

4 Conclusion

The propagation of an 473 nm, continuous wave, laser beam through the synthesized Ethyl (E)-4-((5-hydroxy-3,4-bis(hydroxyl methyl)-6-methyl pyridin-2-yl)diazenyl) benzoate (EAB) compound have generated diffraction patterns which were used together with Z-scan techniques to determine the compound NRI and the NAC. The all-optical switching prove to occur in the prepared compound using two laser beams, controlling and controlled.

Author contributions Qusay M. A. Hassan and Rafid H. Al. Asadi participated in the characterization and analysis of the results, and H. A. Sultan and Hasanain A. Abdullmajed wrote the manuscript, and Asaad A. Ali and C. A. Emshary wrote the main manuscript text–review & editing. All authors reviewed the manuscript."

Funding No funding was received for this study.

Data availability The authors confirm that the data supporting the findings of this study are available within the article.

Declarations

Conflict of interest The authors declare that they have no known competing financial interests or personal relationships that could have appeared to influence the work reported in this paper.

Consent for publication The authors declare their consent of publication.

Ethics approval and consent to participate The authors declare that their commitment to ethics related to his work and they have designed the experiments, collected and analyzed the data, and written the manuscript.

References

Abdel-Kader, N.S., Abdel-Latif, S.A., El-Ansarya, A.L., Sayed, A.G.: Spectroscopic studies, density functional theory calculations, non-linear optical properties, biological activity of 1-hydroxy-4-((4-(N-(pyrimidin-2-yl)sulfamoyl)phenyl)diazenyl)-2-naphthoic acid and its chelates with Nickel (II), Copper (II), Zinc (II) and Palladium (II) metal ions. J. Molec. Struc. **1223**, 129203 (2021)

Abdullmajed, H.A., Sultan, H.A., Al-Asadi, R.H., Hassan, Q.M.A., Ali, A.A., Emshary, C.A.: Synthesis, DFT calculations and optical nonlinear properties of two derived Schiff base compounds from ethyl-4-amino benzoate. Phys. Scr. **97**, 025809 (2022a)

Abu El-Fadl, A., Mohamad, G.A., Abd El-Moiz, A.B., Rashad, M.: Optical constants of Zn1−xLixO films prepared by chemical bath deposition technique. Phys. B **366**, 44–54 (2005)

Agrawal, G.: Modulation, instability induced by cross-phase modulation. Phys. Rev. Lett. **59**, 800–803 (1987)

Al-Asadi, R.H.: Synthesis and molecular structure study of new organotellurium and organomercury compounds based on 4-bromonaphthalen-1-amine. Russ. J. Gen. Chem. **90**, 1744–1749 (2020)

Al-Hamdani, U.J., Hassan, Q.M.A., Emshary, C.A., Sultan, H.A., Dhumad, A.M., Al-Jaber, A.A.: All optical switching and the optical nonlinear properties of 4-(benzothiazolyldiazenyl)-3-chlorophenyl 4-(nonylthio)benzoate (EB-3Cl). Optik **248**, 168196 (2021)

Alharis, R.A., Al-Asadi, R.H., Hassan, D.A.: New mercurated and Tellurated sulpha compounds: synthesis, Invitro anticancer study and DFT calculation. Egypt. J. Chem. **64**, 5755–5764 (2021)

Ali, Q.M., Palanisamy, P.K.: Optical phase conjugation by degenerate four-wave mixing in basic green 1 dye-doped gelatin film using He–Ne laser. Opt. Las. Technol. **39**, 1262–1268 (2007)

Ali, Q.M., Palanisamy, P.K., Manickasundaram, S.P.: Kannan, Sudan IV dye based poly(alkyloxymethacrylate)films for optical data storage. Opt. Commun. **267**, 236–243 (2006)

Ali, H., Majeed, H., Al-Asadi, I., Abdulredha, A., Hussain, A.: Structures effect of two azo dyes associated with their antimicrobial activity, J. Chem. Biolo. Phys. Sci. **8**, 171–185 (2018)
Ali, S.A., Hassan, Q.M.A., Emshary, C.A., Sultan, H.A.: Characterizing optical and morphological properties of Eriochrome Black T doped polyvinyl alcohol film. Phys. Scr. **95**, 095814 (2020)
Al-Masoudi, W.A., Al-Asadi, R.H., Othman, R.M., Al-Masoudi, N.A.: Synthesis, antimicrobial activity, computational and modeling studies of some new organotellurium compounds containing azo moities. Euro. J. Chem. **6**, 374–380 (2015)
Al-Timimy, K.H.A., Qusay, M.A., Hassan, H.A., Sultan, C.A., Emshary: Solvents effect on the optical nonlinear properties of the sudan iv. Optik **224**, 165398 (2020)
Ambs, P.: Optical computing: a 60-year adventure. Adv. Opt. Technol. **2010**, 1–15 (2010). https://doi.org/10.1155/2010/372652
Benkhay, S., Rabet, S.M., El Harfi, A.: Classifications, properties, recent synthesis and applications of azo dyes. Heliyon **6**, e03271 (2020)
Bohac, L.: The soliton transmission in optical fibers. Inf. Commun. Technol. Serv. **8**, 107–110 (2010)
Child, R.G., Wilkinson, R.G., Tomcu-Fucik, A.: Effect of substrate orientation of the adhesion of polymer joints. J. Chem. Soc. **87**, 6031–6038 (1977)
Dadrass, A., Rahchamani, H.: Synthesis of organophosphorus complexes and structural characterization of two dimeric triphenylphosphinne complexes of mercury(II) ions from dimeric complexes of [4-methylbenzoylmethylene tri-p-tolylphosphine mercury(II) halides]. J. Chil. Chem. Soc. **61**, 2968–2972 (2016)
Dhaef, H.K., Al-Asadi, R.H., Shenta, A.A., Mohammed, M.K.: Novel bis maleimide derivatives containing azo group: synthesis, corrosion inhibition, and theoretical study. Indones. J. Chem. **21**, 1212–1220 (2021)
Dhumad, A.M., Hassan, Q.M.A., Tarek Fahad, C.A., Emshary, N., Raheem, A., Sultan, H.A.: Synthesis, structural characterization and optical nonlinear properties of two azo-β-diketones. J. Molec. Struct. **1235**, 130196 (2021a)
Dhumad, A.M., Qusay, M.A., Hassan, C.A.E., Fahad, T., Raheem, N.A., Sultan, H.A.: Nonlinear optical properties investigation of a newly synthesised Azo-(β)-diketone dye. J. Photochem. Photobio. A Chem. **418**, 113429 (2021b)
Elias, R.S., Hassan, Q.M.A., Sultan, H.A., Al-Asadi, A.S., Saeed, B.A., Emshary, C.A.: Thermal nonlinearities for three curcuminoids measured by diffraction ring patterns and Z-scan under visible CW laser illumination. Opt. Las. Technol. **107**, 131–141 (2018)
Elias, R.S., Hassan, Q.M.A., Emshary, C.A., Sultan, H.A., Saeed, B.A.: Formation and temporal evolution of diffraction ring patterns in a newly prepared dihydropyridone, Spectroch. Acta Part A Molec. Biomol. Spec. **223**, 117297 (2019)
Emshary, C.A., Ali, I.M., Hassan, Q.M.A., Sultan, H.A.: Linear and nonlinear optical properties of potassium dichromate in solution and solid polymer film. Phys. B **613**, 413014 (2021a)
Emshary, C.A., Hassan, Q.M.A., Bakr, H., Sultan, H.A.: Determination of the optical constants, nonlinear optical parameters and threshold limiting of methyl red-epoxy resin film. Phys. B **622**, 413354 (2021b)
Farghaly, T.A., Abdallah, Z.A.: Synthesis, azo-hydrazone tautomerism and antitumor screening of *N*-(3-ethoxycarbonyl 4, 5, 6, 7-tetrahydro-benzo[b]thien-2-yl)-2-arylhydrazono-3-oxobutanamide derivatives. ARKIVOC **17**, 295–305 (2008)
Fayadh, R.H., Ali, A.A., F. M. Al–Jabri,: Synthesis and identification symmetrically azo dyes derived from sulfa compounds and spectrophotometric study of nickel (II) complexes with prepared dyes. IJETR **3**, 25–28 (2015)
Ghanavatkar, C.W., Mishra, V.R., Sharma, S., Mathew, E., Chitrambalam, S., Joe, I.H., Nethi, S.N.: Red Emitting Hydroxybenzazole (HBX) based azo dyes: linear and non linear optical properties, optical limiting, z scan analysis with DFT assessments. J. Fluor. **30**, 335–346 (2020)
Jassem, A.M., Qusay, M.A., Hassan, C.A., Emshary, H.A., Sultan, F.A., AlmashalRadhi, W.A.: Synthesis and optical nonlinear properties performance of azonaphthol dye. Phys. Scr. **96**, 025503 (2021)
Jia, Y., Shan, Y., Wu, L., Dai, X., Fan, D., Xiang, Y.: Broad band nonlinear optical resonance and all-optical switching of liquid phase exfoliated tungsten diselenide. Phot. Res. **6**, 1040–1046 (2018)
Jia, Y., Liao, Y., Leiming, Wu., Shan, Y., Dai, X., Cai, H., Xiang, Y.: Dianyuan Fan Nonlinear optical response, all optical switching, and all optical information conversion in NbSe2 nanosheets based on spatial self-phase modulation. Nanoscale **11**, 4515–4522 (2019)
Jones, D.J., Diddams, S.A., Taubman, M.S., Cundiff, S.T., Ma, L.-S., Hall, J.L.: Frequency comb generation using femtosecond pulses and cross-phase modulation in optical fiber at arbitrary center frequencies. Opt. Lett. **25**, 308–310 (2000)

Khalaf, S.K., Hassan, Q.M.A., Emshary, C.A., Sultan, H.A.: Concentration effect on optical properties and optical limiting of PVA doped with nigrosin films. J. Photochem. Photobio. A Chem. **427**, 113809 (2022)

Kirkan, B., Gup, R.: Synthesis of new azo dyes and copper (II) complexes derived from barbituric acid and 4-aminobenzoylhydrazone. Turk. J. Chem. **32**, 9–17 (2008)

Langhals, H: Color chemistry; synthesis, properties and Application of organic dyes and pigments , 3rd revised edition, Book Review, (2004)

Manickasundaram, S., Kannan, P., Qusay, M.A., HassanPalanisamy, P.K.: Azo dye based poly(alkyloxymethacrylate)s and their spacer effect on optical data storage. J Mater. Sci: Mater. Electron. **19**, 1045–1053 (2008a)

Manickasundaram, S., Kannan, P., Hassan, Q.M.A., Palanisamy, P.K.: Holographic grating formation in poly(methacrylate) containing pendant xanthene dyes. Optoelec. Adv. Mater. Rap. Commun. **2**, 324–331 (2008b)

Manickasundaram, S., Kannan, P., Kumaran, R., Velu, R., Ramamurthy, P., Qusay, M.A., Hassan, P.K., Palanisamy, S., SenthilNarayanan, S.S.: Holographic grating studies in pendant xanthene dyes containing poly(alkyloxymethacrylate)s. J. Mat. Sci. Mat. Electron. **22**, 25–34 (2011)

Matsuoka, S., Miyanaga, N., Amano, S., Nakaosuka, M.: Frequency modulation controlled by cross-phase modulation in optical fiber. Opt. Lett. **22**, 25–276 (1997)

Mishra, A.K., Tewari, S.P.: 7-Hydroxy-6-methoxy-coumarian to be a multifunctional bioactive natural molecule: a theoretical study. Mater. Tod. Proc. **15**, 400–408 (2019)

Mohammed, H.: Synthesis, identification, and biological study for some complexes of azo dye having theophylline. Sci. Wor. J. **2021**, 1–9 (2021)

Mutlaq, D.Z., Hassan, Q.M.A., Sultan, H.A., Emshary, C.A.: The optical nonlinear properties of a new synthesized azo-nitrone compound. Opt. Mater. **113**, 110815 (2021)

Ogusu, K., Kohtani, Y., Shao, H.: Laser-induced diffraction rings from an absorbing solution. Opt. Rev. **3**, 232–234 (1996)

Otutu, J.O.: Synthesis and application of azo dyes derived from 2-amino-1, 3,4-thiadiazole-2-thiol on polyester fibre. IJRRAS **15**, 292–296 (2013)

Qusay, M.A., Hassan, C.A., Emshary, H.A., Sultan,: Investigating the optical nonlinear properties and limiting optical of eosin methylene blue solution using a cw laser beam. Phys. Scr. **96**, 095503 (2021)

Ruddock, I.S.: Nonlinear optical harmonic generation. Eur. J. Phys. **15**, 53–58 (1994)

Saeed, B.A., Hassan, Q.M.A., Emshary, C.A., Sultan, H.A., Elias, R.S.: The nonlinear optical properties of two dihydropyridones derived from curcumin, Spectrochim. Acta Part A Molec. Biomol. Spec. **240**, 118622 (2020)

Shabeeb, G.M., Emshary, C.A., Hassan, Q.M.A., Sultan, H.A.: Investigating the nonlinear optical properties of poly eosin-Y phthalate solution under irradiation with low power visible CW laser light. Phys. B **578**, 411847 (2020)

Shan, Y., Tang, J., Wa, L., Ln, S., Dain, X.: Spatial self-phase nodulation and all-optical switching of graphene oxciz dimensional martials. J. Cent. South Univ. **26**, 2295–2306 (2014)

Sheik-Bahae, M., Said, A.A., Van Stryland, E.W.: High sensitivity single beam n_2 measurements. Opt. Lett. **14**, 955–957 (1989)

Sheik-Bahae, M., Said, A.A., Wei, T., Hagan, D.J., Van Stryland, E.W.: Sensitive measurement of optical nonlinearities using a single beam. IEEE J. Quant. Electron. E **26**, 760–769 (1990)

Shen, Y., Tang, J., Wu, L., Lu, S., Dai, X., Xiang, Y.: Spatial self-phase modulation and all-optical switching of grapheme oxide dispersions. J. Allo. Comp. **771**, 900–904 (2019)

Sidir, Y.G., Sidir, I., Berber, H., Tasal, E.: UV-spectral changes for some azo compounds in the presence of different solvents. J. Molec. Liq. **162**, 148–154 (2011)

Sultan, H.A., Dhumad, A.M., Hassan, Q.M.A., Tarek Fahad, C.A., Emshary, N.A., Raheem,: Synthesis, characterization and the nonlinear optical properties of newly synthesized 4-((1,3-dioxo-1-phenylbutan-2-yl)diazenyl) benzenesulfonamide, Spectroch. Act. Part A Mole. Biomolec. Spec. **251**, 119487 (2021)

Tahir, T., Ashfaq, M., Saleem, M., Rafiq, M., Imran Shahzad, M., Kotwica-Mojzych, K., Mojzych, M.: Pyridine scaffolds, phenols and derivatives of azo moiety: curr. Therap. Perspe. Molec. **26**, 4871–4888 (2021)

Villafranca, A.B., Saravanamuttu, K.: Diversity and slow dynamics of diffraction ring patterns:a comprehensive study of spatial self-phase modulation in a photopolymer. J. Opt. Soc. Am. B **29**, 2357–2372 (2012)

Zhang, X.J., Yuan, Z.H., Yang, R.X., He, Y.I., Qin, Y.I., Xiao, S., He, J.: A review on spatial self-phase modulation of two dimensional materials. J. Cet. South Univ. **26**, 2295–2306 (2019)